PAPER

Aggregates of polar dyes: beyond the exciton model†

Mattia Anzola and Anna Painelli (ID) *

The physics of aggregates of polar and polarizable donor–acceptor dyes is discussed, extending a previous model to account for the coupling of electronic and vibrational degrees of freedom. Fully exploiting translational symmetry, exact absorption and fluorescence spectra are calculated for aggregates with up to 6 molecules. A two-step procedure is presented: in the first step, a mean-field solution of the problem is proposed to define the excitonic basis *via* a rotation of the electronic basis. The rotation is also accompanied by a Lang–Firsov transformation of the vibrational basis. In the second step, the aggregate Hamiltonian, written on the exciton basis, is diagonalized towards exact results. The procedure leads to a reduction of the dimension of the problem, since, at least for weak coupling, only states with up to 3 excitons are needed to obtain reliable results. More interestingly, the mean-field solution represents the proper reference state to discuss excitonic and ultraexcitonic effects. The emerging picture demonstrates that the exciton model offers a reliable description of aggregates of polar and polarizable dyes in the weak coupling regime, while ultraexcitonic effects are important in the medium-strong coupling regimes, and particularly so for J-aggregates where ultraexcitonic effects show up most clearly with multistability and multiexciton generation.

1 Introduction

Electrostatic intermolecular interactions are comparatively weak forces in supramolecular systems, but they are responsible for energy transfer, an incoherent process where energy is transferred between different chromophores,[1–4] as well as for the coherent process of energy delocalization that governs the spectral properties of molecular crystals and aggregates.[5–7] Typically, energy transfer processes are investigated in loosely bound systems with intermolecular distances larger than ~10 Å,[8,9] whereas in molecular crystals and aggregates fairly compact structures are of interest with intermolecular distances comprised roughly in the 3.5–7 Å range. In some systems, including molecular crystals as well as aggregates, intermolecular charge transfer (CT) interactions are important,[10–13] but here we will only discuss systems where CT interactions can be safely neglected, or, in other words, aggregates where electrons are localized in each molecular unit.[5,6,14,15]

The exciton model, widely adopted to describe the optical spectra of molecular crystals and aggregates, dates back to the 1960s[5,14–16] and has found several successful applications, as recently extensively reviewed by Spano.[7,17] In the simplest version, it accounts for a single excitation on each molecule and, neglecting

electrostatic interactions among non-degenerate states, reduces the problem to that of a single particle, the exciton, moving on the molecular lattice. The corresponding problem is easily solved even on fairly large aggregates and, for symmetric (crystalline-like) systems, exact solutions in the thermodynamic limit are also available. Davydov splittings in crystals[15] and J and H-bands in aggregates[14] emerge quite naturally from this picture that can also be extended to discuss the chirooptical properties of chiral aggregates.[18–20]

Molecules are flexible objects and their geometry usually responds to electronic excitations, as demonstrated by the prominent Frank–Condon structures often observed in molecular spectra. Extending the exciton model to account for molecular vibrations is non-trivial, mainly because the adiabatic (or Born–Oppenheimer) approximation cannot be applied. Indeed there are two easy limits: the vibrational frequency is either (a) much smaller or (b) much higher than the hopping frequency of the exciton. Case (a) corresponds to the adiabatic limit: the molecule has no time to relax its geometry following the exciton motion and vibrational coupling does not affect the optical spectra. Case (b) corresponds to the antiadiabatic limit:[21] the exciton is trapped in the molecular site and the optical spectra show the same vibronic structure as the isolated molecule. Between these two limits the problem becomes non-adiabatic and special techniques must be adopted for its solution.[17,22] Quite interestingly, interpolating between the two limits, the vibronic structure observed in the aggregate can lead to a reliable estimate of the exciton delocalization, as first proposed by Spano.[23]

Department of Chemistry, Life Science and Environmental Sustainability, University of Parma, 43124 Parma, Italy. E-mail: anna.painelli@unipr.it

† Electronic Supplementary Information (ESI) available: Detailed derivation of the Hamiltonian in the exciton basis; additional computational results. See DOI: 10.1039/d1cp00335f

8282 | *Phys. Chem. Chem. Phys.*, 2021, **23**, 8282–8291

This journal is © the Owner Societies 2021

Neglecting the interactions between non-degenerate states, the exciton model does not account for the effect of the local environment on the molecular properties, including *e.g.* the charge distribution in the ground or excited states, the transition energy and dipole moment *etc.* Typically, the parameters entering the exciton model, *i.e.* the reference transition frequency and the transition dipole moment, are obtained from the analysis of experimental data on isolated (solvated) molecules, thus implicitly accounting for environmental corrections. Indeed the environmental polarity has marginal effects in non-polar dyes, whereas the medium polarizability can be considered roughly constant for organic media.[24] Extracting the same quantities from quantum chemical calculations in the gas phase is trickier. Most often, reference transition frequencies are empirically adjusted.[15,16] Deviations from the exciton model are mainly recognized in the intensity of optical transitions as well as of CD spectra.[25] However, in aggregates of non-polar dyes with a large quadrupolar character, large deviations from the exciton model are observed:[26–30] in these systems, the dense excitation spectrum at the molecular level, and the large molecular polarizability, make the approximations of the exciton model critical, with impressive effects on linear and nonlinear optical spectra.

Even more intriguing is the situation in aggregates of polar dyes.[31,32] Indeed, as long as the molecular polarizability stays small, the exciton model, possibly with marginal corrections, still applies. However, in clusters of polar and polarizable dyes, typically push–pull dyes with large conjugation and hence strongly polarizable structures,[33] large deviations from the easy predictions of the exciton model are expected. Push–pull chromophores are π-conjugated molecules with an electron donor (D) and an acceptor (A) unit, whose low-energy physics is dominated by the charge resonance between a neutral DA (N) and a zwitterionic (Z) D^+A^- structure.[34–36] The resulting two-state model accounts for both the molecular polarity and polarizability and very interesting physics emerges when clusters of dyes are considered, interacting *via* electrostatic intermolecular interactions. The model for interacting polar and polarizable dyes was introduced more than 40 years ago by Soos, as a toy model to describe the neutral-ionic phase transition in mixed stack CT crystals.[37] Multistability was recognized and has been discussed since then in different systems,[38–40] and spectroscopic effects in clusters of polar and polarizable molecules were also addressed.[31,32,41–43]

The number of basis states needed to describe aggregates of polar and polarizable dyes, increases as 2^N, N being the number of molecules. The relevant Hamiltonian can be diagonalized on fairly large systems.[31] Accounting for vibrational coupling however is challenging and so far exact solutions are only available for dimers,[41] whereas for larger systems, dramatic approximations have been introduced.[42] In a recent paper, Spano analyzed in detail the absorption spectra of dimers of push–pull dyes fully accounting for vibrational coupling.[43] An interesting discussion of spectral bandshapes emerges together with the demonstration of dramatic deviation from the Kasha behavior. In this paper we face the same problem, adopting the exciton transformation described in ref. 31, and a Lang–Firsov transformation for the vibrational coupling.[21] An optimized

basis set with reduced dimension can then be defined, and, fully accounting for symmetry, we can handle comparatively large systems with up to 6 molecules. On a different perspective, the exciton transformation helps us to disentangle meanfield effects from excitonic and ultraexcitonic effects in these systems. Indeed, for weakly interacting aggregates, the Kasha model works well, provided the proper mean-field reference state is selected. On the other hand, in the case of attractive interactions and strong coupling, multistability is expected and wild spectroscopic effects are observed, definitely beyond any exciton-like description.

2 The model

Each DA dye is described by two electronic diabatic states, corresponding to the two limiting neutral and zwitterion structures, $|N\rangle$ and $|Z\rangle$, respectively (Fig. 1). The two electronic states are separated by an energy gap $2z_0$ and are mixed by a matrix element $-\tau$. To account for the different geometry of the molecule in the two diabatic states, a single harmonic vibration with – frequency ω_v is considered on each molecular unit, leading to a linear dependence of the energy gap between the basis states on the coordinate, as shown by the diabatic potential energy curves in Fig. 1c.[34]

The Hamiltonian for an aggregate of N equivalent dyes, only interacting *via* electrostatic interactions, reads:

$$\mathcal{H} = \sum_i \left\{ \left[2z_0 - g\left(\hat{a}_i^\dagger + \hat{a}_i\right) \right] \hat{\rho}_i - \tau \sigma_i + \hbar \omega_v \left(\hat{a}_i^\dagger \hat{a}_i + \frac{1}{2} \right) \right\}$$
$$+ \sum_{i>j} V_{ij} \hat{\rho}_i \hat{\rho}_j$$

$$(1)$$

where i and j run on the molecular sites. The terms in the curly bracket define the molecular Hamiltonian and $\hat{\rho}_i = |Z\rangle_i \langle Z|_i$
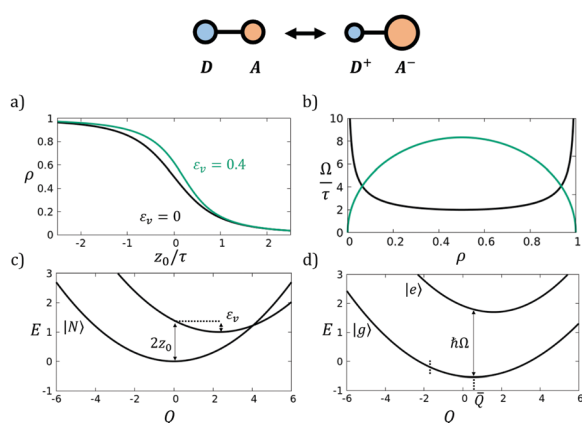

Fig. 1 The isolated (gas-phase) dye. Top: The two resonating structures. (a) The $\rho(z_0/\tau)$ curves calculated for $\varepsilon_v = 0$ and 0.4τ. (b) The transition energy Ω and the transition dipole moment as a function of ρ. (c) The potential energy surfaces for a system with $\tau = 1$, $\varepsilon_v = 0.4$ and $z_0 = 0.7$. (d) The adiabatic PES calculated for the same system as in panel (c).

This journal is © the Owner Societies 2021

Phys. Chem. Chem. Phys., 2021, **23**, 8282–8291 | **8283**

measures the weight of the zwitterionic state in the i-th molecule, $\hat{\sigma}_i = |Z\rangle_i\langle N|_i + |N\rangle_i\langle Z|_i$, and $\hat{a}_i$ is the distruction operator for a vibrational quantum on the i-th molecule, so that the vibrational coordinate and its conjugated momentum are:

$$Q_i = \sqrt{\frac{\hbar}{2\omega_v}}\left(\hat{a}_i^\dagger + \hat{a}_i\right)$$

$$P_i = i\sqrt{\frac{\hbar\omega_v}{2}}\left(\hat{a}_i^\dagger - \hat{a}_i\right) \quad (2)$$

Finally, g is the electron-vibration coupling constant, related to the vibrational relaxation energy as $\varepsilon_v = g^2/(\hbar\omega_v)$, as shown in Fig. 1c. Specifically ε_v measures the energy gained by the molecule due to its geometrical rearrangement when its state changes from N to Z. The last term in eqn (1) accounts for intermolecular electrostatic interactions with V_{ij} measuring the interaction between molecules on site i and j when both molecules are in a zwitterionic state. In the following, we will only account for nearest neighbor interactions, even if extending the calculation to more general forms of the electrostatic potential is trivial. Moreover, we will impose periodic boundary conditions and will consider systems with just one molecule per unit cell. Finally, for the sake of simplicity, we will consider aligned molecules, so that only two limiting structures are of interest, as shown in Fig. 2. Since intermolecular interactions are attractive and repulsive in the two structures we dub them as J and H-structures, respectively.

Essential state models are traditionally parametrized from a detailed analysis of optical spectra (typically absorption and fluorescence) collected in solvents of different polarity, as to disentangle the effect of environmental polarity, but fully accounting for the environmental polarizability.[35,36,42,44] Under the assumption that the environmental polarizability (as measured
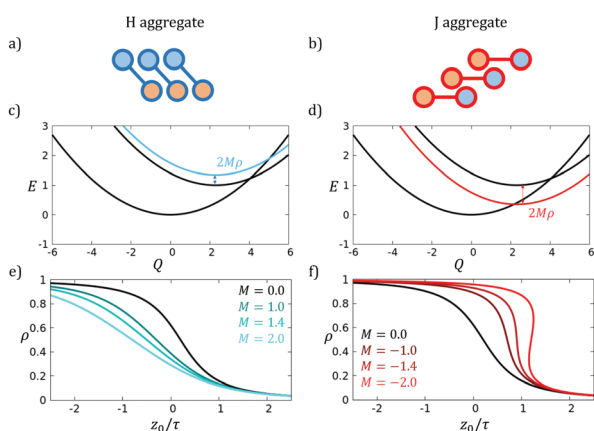

Fig. 2 The mf solution. Panels (a) and (b) show the H and J geometries, respectively. (c) The diabatic PES for the isolated dye and for a dye in an H-aggregate. (d) The diabatic PES for the isolated dye and for a dye in a J-aggregate. (e) The $\rho(z_0/\tau)$ curves calculated for an H aggregate with $M = 0$ (isolated dye) and $M = 1$. (f) The $\rho(z_0/\tau)$ curves calculated for a J aggregate with $M = 0$ (isolated dye) and $M = -1$, -1.4 and -2.0. All results refer to systems with $\varepsilon_v = 0.4\tau$.

e.g. by the medium refractive index) is similar in all organic media, the resulting effective model should properly account for the core polarizability of the surrounding molecules in the aggregate, i.e. of the polarizability due to the electronic degrees of freedom not explicitly included in the molecular essential state model. Extracting the same information from quantum chemical calculations is possible, but gas-phase results must be properly corrected to account for the environmental polarizability.[45]

2.1 Rotating the basis

The Hamiltonian in eqn (1) can be written on the basis obtained as the direct product of the 2^N electronic basis states multiplied by the states (at least the first few states) of each molecular harmonic oscillator. Even accounting for just 5 vibrational states on each oscillator, the basis, growing as 10^N, explodes very fast with N. The adopted diabatic basis leads to a very simple expression for the Hamiltonian describing the aggregate, but it is not the most clever basis. Indeed we need to account for all electronic states and for a large number of vibrational states simply to be able to recover a reliable description of the molecular ground state in terms of charge distribution and equilibrium geometry.

As discussed in ref. 31 the molecular electronic basis can be rotated from the diabatic to the exciton basis $|g\rangle$, $|e\rangle$ via the transformation:

$$|g\rangle = \sqrt{1-\rho}|N\rangle + \sqrt{\rho}|Z\rangle$$

$$|e\rangle = \sqrt{\rho}|N\rangle - \sqrt{1-\rho}|Z\rangle \quad (3)$$

where the parameter ρ, between 0 and 1, measures the weight of the zwitterionic state into the $|g\rangle$ state, a measure of the molecular polarity. A clever choice sets ρ to the mean-field (mf) result: when inserted in the aggregate, each dye feels the electrostatic potential generated by the surrounding molecules, and readjusts its ground state ionicity in response to this potential. The potential in turn depends on the ionicity of the molecules, leading to a self-consistent problem, which has been solved and discussed many times.[11,31,37]

However, the mean field ionicity is also affected by the vibrational coupling. For each molecule, the Hellman–Feynman theorem sets the equilibrium coordinate proportional to ρ as follows (see ESI† for explicit expressions):[38]

$$\bar{Q}_i = \sqrt{\frac{2\omega_v}{\hbar}}\frac{g}{\omega_v^2}\rho \quad (4)$$

It is convenient to move the origin of the vibrational coordinate to the equilibrium position, via a Lang–Firsov transformation of the vibrational operators:[21]

$$\hat{\tilde{Q}}_i = \hat{Q}_i - \bar{Q} = \sqrt{\frac{\hbar}{2\omega_v}}\left(\hat{\tilde{a}}_i^\dagger + \hat{\tilde{a}}_i\right)$$

$$\hat{\tilde{P}}_i = \hat{P}_i = i\sqrt{\frac{\hbar\omega_v}{2}}\left(\hat{\tilde{a}}_i^\dagger - \hat{\tilde{a}}_i\right) \quad (5)$$

Applying the exciton rotation to the electronic basis and the Lang–Firsov transformation to the molecular oscillators, the

8284 | Phys. Chem. Chem. Phys., 2021, 23, 8282–8291

This journal is © the Owner Societies 2021

Hamiltonian in eqn (1) reads (the derivation can be found in ESI†):

$$\mathscr{H} = \hbar\Omega \sum_i \hat{n}_i + \hbar\omega_v \sum_i \left(\hat{\tilde{a}}_i^\dagger \hat{\tilde{a}}_i + \frac{1}{2} \right)$$

$$- g\left[(1-2\rho) \sum_i \hat{n}_i \left(\hat{\tilde{a}}_i^\dagger + \hat{\tilde{a}}_i \right) \right.$$

$$\left. + \sqrt{\rho(1-\rho)} \sum_i \left(\hat{b}_i^\dagger + \hat{b}_i \right) \left(\hat{\tilde{a}}_i^\dagger + \hat{\tilde{a}}_i \right) \right]$$

$$+ \sum_{i>j} V_{ij}\rho(1-\rho) \left[\left(\hat{b}_i^\dagger \hat{b}_j + \hat{b}_j^\dagger \hat{b}_i \right) + \left(\hat{b}_i^\dagger \hat{b}_j^\dagger + \hat{b}_j \hat{b}_i \right) \right]$$

$$+ (1-2\rho)^2 \sum_{i>j} V_{ij}\hat{n}_i\hat{n}_j + 2\sqrt{\rho(1-\rho)}(1-2\rho) \sum_{i>j} \hat{n}_i \left(\hat{b}_j^\dagger + \hat{b}_j \right)$$

$$(6)$$

The Paulion operator $\hat{b}_i^\dagger$ creates and exciton at site i, bringing the relevant molecule from the $|g\rangle$ state (the vacuum state) to the excited $|e\rangle$ state. The number operator $\hat{n}_i = \hat{b}_i^\dagger \hat{b}_i$ counts the number of excitons on site i (0 for g, 1 for e states).

The above Hamiltonian is exactly equivalent to the Hamiltonian in eqn (1), provided ρ is fixed to the mean field value:[31]

$$\rho = \frac{1}{2} - \frac{z(\rho)}{2\sqrt{z(\rho)^2 + \tau^2}} \qquad (7)$$

where $z(\rho)$ measures half the energy gap between the two diabatic states that self-consistently depends on ρ:

$$z(\rho) = z_0 + (M - \varepsilon_v)\rho \qquad (8)$$

where M defines the Madelung energy

$$M = \frac{1}{N} \sum_{i>j} V_{ij} \qquad (9)$$

that reduces to $M = V$ when only the nearest neighbor interactions are considered.

To understand the physical picture that emerges from the aggregate Hamiltonian on the rotated basis (eqn (6)), we first address the mf solution for the aggregate. To start with, for an isolated molecule in the gas phase and neglecting the vibronic coupling ($\varepsilon_v = 0$), the solution of the two-dimensional electronic problem is trivial and leads to the $|g\rangle$ and $|e\rangle$ states in eqn (3) with ρ fixed by eqn (7) but with $z = z_0$. The $|g\rangle \rightarrow |e\rangle$ transition energy and transition dipole moment are expressed as a function of ρ as follows:[34]

$$\hbar\Omega = \frac{\tau}{\sqrt{\rho(1-\rho)}}$$
$$\mu_{ge} = \mu_0 \sqrt{\rho(1-\rho)} \qquad (10)$$

where μ_0 is the dipole moment associated with the zwitterionic state, proportional to the intramolecular D–A distance. The $\rho(z_0)$ curves and the ρ-dependence of the transition energy and dipole moments of the isolated dye are shown in Fig. 1a and b.

When accounting for vibronic coupling, the energies of the diabatic states acquire a Q-dependence, as shown for typical model parameters in Fig. 1c. In the adiabatic approximation, the two-dimensional electronic Hamiltonian is diagonalized for each Q to get the adiabatic potential energy curves for the $|g\rangle$ and $|e\rangle$ states, shown in Fig. 1d. If we are only interested in adiabatic results for the equilibrium $Q = \bar{Q}$, we may exploit eqn (4) and solve the self-consistent two-dimensional adiabatic Hamiltonian for a system where the energy difference between the diabatic states self-consistently depends on ρ as $2z = 2z_0 - 2\varepsilon_v\rho$.[38,40] While the equilibrium ρ is affected by the vibrational coupling, the ρ-dependence of the transition frequency and dipole moment is always defined by eqn (10), so that the curves in Fig. 1b apply irrespective of the ε_v value.

When the dye is inserted in the aggregate its ionicity will readjust in response to the surrounding charges. In an H-type (repulsive) geometry (Fig. 2a), the ionicity of the dye in the aggregate will be lower than for the isolated dye, whereas in a J-type (attractive) geometry it will be higher. The calculation is easy in the mf approximation: each molecule feels the electrostatic potential generated by the surrounding molecules, each one bearing a fractional charge $\pm\rho$ at the D/A site. The energy of the zwitterionic state is then moved with respect to the isolated molecule by a quantity $2M\rho$, positive and negative for H and J aggregates, respectively (see Fig. 2c and d). The mf solution of the problem is then obtained self-consistently, setting the ionicity of the surrounding molecules equal to the ionicity of the test molecule, then regaining eqn (7). The $\rho(z_0)$ curves in Fig. 2(e) and (f) are calculated accordingly. Of particular interest is the case of J-aggregates, where not only does the molecular ionicity increase with M, as expected, but, at large enough M values, a discontinuous behavior emerges,[31,38,39] with sizable bistability regions. Once again, the molecular ionicity is affected by the interactions, but the ρ-dependence of the transition dipole moment and frequency are fixed as in eqn (10).

Having described the mf solution, we are now in a position to discuss the rotated Hamiltonian in eqn (6). The first line assigns energy $\hbar\Omega$ to each exciton and adds the vibrational energy $\hbar\omega_v$ to each vibrational excitation. The second and third lines account for the vibrational coupling. As expected, it is an on-site term. The first term in these lines is the standard Condon term, with the vibrational coupling renormalized from g to $g(1 - 2\rho)$ to account for the relative position of the equilibrium geometries for the ground and excited state potential energy surfaces (PES).[46] The second term (third line) is instead an ultraexcitonic term mixing states with the number of excitons differing by one unit. This ultraexciton term has a vibronic origin: the creation/destruction of the exciton on site i is always accompanied by the creation or destruction of a vibrational quantum in the same site. The terms in the two last lines of eqn (6) all come from intermolecular electrostatic interactions. The term in the fourth line is proportional to the squared transition dipole moment of the mf dye (see eqn (10)) and contains both the exciton hopping term, as well as the two-exciton terms that are usually neglected in the exciton model.[25] In the last line the first term is an exciton–exciton interaction

term (proportional to the squared mesomeric moment): it conserves the exciton mumber and it may enter the exciton model, but is of course relevant only to aggregates of polar dyes.[31] The very last term is again an ultraexcitonic term mixing states whose exciton number changes by one unit.

A special situation occurs in the so-called cyanine limit, when the mean field ρ reaches a value of 0.5. This occurs whenever $z(\rho = 0.5) = 0$ in eqn (8), or $2z_0 - \varepsilon_v = M$ (or $2z_0 - \varepsilon_v = V$, for nearest neighbor interactions), fully in line with the analogous result for a dimeric aggregate in ref. 43. In the cyanine limit, the leading Condon term for vibronic coupling vanishes, and the vibronic structure in aggregate spectra is washed out,[43] with marginal vibronic effects only expected for strong coupling, when the ultraexcitonic term enters into play. Moreover, all excitonic and ultraexcitonic terms proportional to $(1 - 2\rho)$ (*i.e.* to the mesomeric dipole moment) vanish when $\rho = 0.5$ so that only terms proportional to the squared transition dipole moment survive. In the cyanine limit then the electronic part of the Hamiltonian in eqn (6) reduces to the Hamiltonian for aggregates of non-polar dyes.[25]

2.2 Computational strategy

The dimension of the non-adiabatic basis increases fast with the aggregate dimension. On each molecular unit the basis includes 2 electronic states to be multiplied by the number of vibrational states as needed for convergence, n_{ph}. The basis for an aggregate of N molecules then has the dimension $(2n_{ph})^N$, quickly leading to intractable problems. To overcome this limitation, we make use of symmetry: the adopted periodic boundary conditions in fact not only help to minimize finite size effects, but also enforce translational symmetry in the system. The wavevector k is then a good quantum number for the aggregate, with optical transitions obeying a strict selection rule imposing that only states with the same wavevector can be reached. The ground state is a zero-wavevector state, so that only the $k = 0$ subspace is of interest for absorption processes. In J-aggregates the lowest excited state also has $k = 0$, so that, again, only the $k = 0$ subspace is of interest. In H-aggregates instead the lowest excited state belongs to the $k = \pi$ subspace, so that, to address fluorescence in H-aggregates, we must also diagonalize the model Hamiltonian in the $k = \pi$ subspace.

To further reduce the dimension of the problem we work in the exciton basis that, while leading to a fairly cumbersome Hamiltonian, allows, for intermolecular interactions that are not too large, to limit the basis dimension discarding all states with a number of excitations larger than M_e with $M_e \leq N$. Moreover, we truncate the vibrational basis so as to discard all states with a total number of vibrational quanta larger than M_v. Of course, large enough M_e and M_v must be considered to ensure convergence on relevant results.

In the bit-representation, we store each basis state in the computer memory as an integer number whose binary code is composed of 4 bits for each molecule in the aggregate, where the first bit represents the electronic state ($0 \equiv |g\rangle$, $1 \equiv |e\rangle$) and the following 3 bits store the integer number that counts the vibrational quanta (from a minimum of $000 \equiv |0\rangle$ to a

maximum of $111 \equiv |7\rangle$). The basis set is created scrolling through all integer numbers from 0 to 16^{N-1} and selecting only the states that comply with the required values of M_e and M_v. Translational symmetry operations are then applied to the basis states to finally obtain symmetry-adapted linear combinations in the $k = 0$ space, as needed to calculate spectra of J and H-aggregates, and in the $k = \pi$ subspace for H-aggregates to address their fluorescence spectra. Since the basis is very large, we only store a single representative state for each symmetry-adapted linear combination, together with the information concerning its multiplicity. The Hamiltonian in eqn (6) is finally written on the symmetrized basis and diagonalized in the relevant subspaces. Depending on the number of excitons and vibrational states needed to reach convergence, we are able to address systems with up to $N = 6$ sites (of course only aggregates with an even N can be considered in the $k = \pi$ subspace).

3 Results

In the following we set $\tau = 1$ as the energy unit (typical values for CT dyes are of the order of 1 eV, even if for dyes of interest for thermally activated delayed fluorescence[47] τ can be up to an order of magnitude smaller), and fix $\varepsilon_v = 0.4$ and $\omega_v = 0.17$. Results will be shown for different z_0 so as to decribe the properties of dyes with different ionicities. All results were obtained setting $N_v = 6$.

3.1 Weak coupling

We start our analysis with H-aggregates, setting a moderate value for the electrostatic interaction, $V = 1$. Fig. 3 shows results for a largely neutral dye, a dye with intermediate ionicity and a zwitterionic dye. Results are shown for the biggest achievable aggregate $N = 6$, but finite size effects are negligible in this case. Convergence is obtained already for $N_e = 3$, as the $N_e = 3$ and 4 results are superimposed in the scale of the figure. In all cases, in line with the H-nature of the aggregate, as determined by repulsive intermolecular interactions, the fluorescence intensity is largely suppressed as a result of aggregation, and a huge Stokes shift is observed for the aggregate. Understanding the position of absorption bands is however tricky. With reference to the isolated (gas phase) dye, the absorption band blueshifts for the dyes with low and intermediate polarity (left and central panels), but red-shifts in the case of a largely polar dye (right panel). These apparently crazy results, possibly suggesting the failure of the exciton picture, are indeed related to a bad choice of the reference state. A large part of the shift in fact is not excitonic in origin, but is related to the effects that surrounding charges have on the energy of the states. This is easily calculated in the mf approximation. Repulsive intermolecular interactions reduce the polarity of each dye in the aggregate (see Fig. 2e), hence affecting the frequency of the absorption band. The proper reference for the exciton model is indeed represented by the mf absorption frequency. Specifically, for the dye in the left panels of Fig. 3, the ionicity decreases from 0.19 in
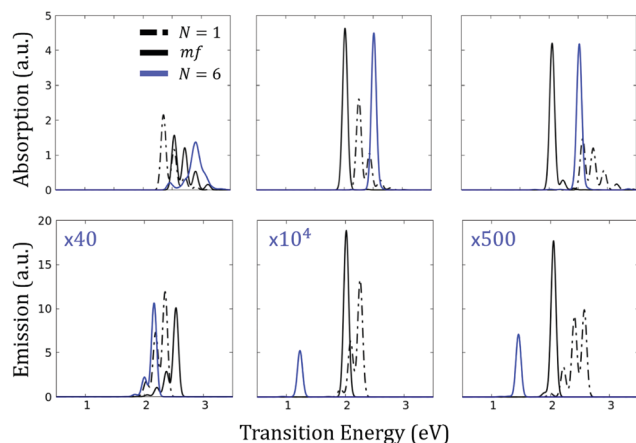
Fig. 3 H aggregate, $V = 1$, $\varepsilon_v = 0.4$, $\omega_v = 0.17$: top and bottom panels show the calculated absorption and fluorescence spectra, respectively. Intensities per molecule are reported in arbitrary units. The weak florescence spectra of the aggregate are multiplied by a factor, as shown in the figure. Left panels refer to a system with $z_0 = 0.8$, corresponding to an ionicity for the isolated dye $\rho = 0.21$ that deacreses in the mf approximation to $\rho = 0.17$. Middle panels: $z_0 = -0.3$, gas phase $\rho = 0.76$, mf $\rho = 0.5$. Right panels: $z_0 = -0.6$, gas phase $\rho = 0.84$, mf $\rho = 0.61$.
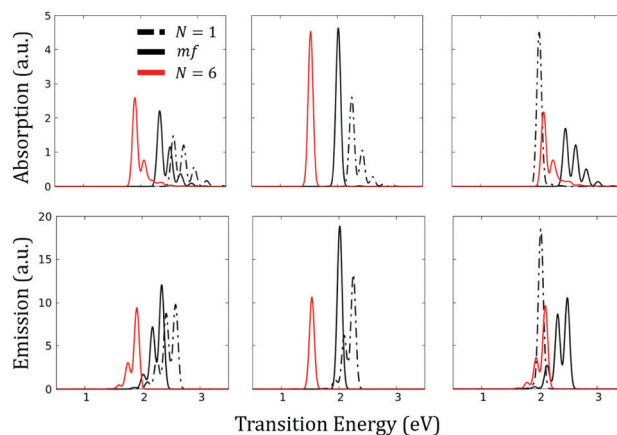

Fig. 4 J aggregate, $V = -1$, $\varepsilon_v = 0.4$, $\omega_v = 0.17$: top and bottom panels show the calculated absorption and fluorescence spectra, respectively. Intensities per molecule are reported in arbitrary units. Left panels refer to a system with $z_0 = 1.0$, corresponding to an ionicity for the isolated dye $\rho = 0.15$ that increases in the mf approximation to $\rho = 0.21$. Middle panels: $z_0 = 0.7$, gas phase $\rho = 0.21$, mf $\rho = 0.50$. Right panels: $z_0 = 0.3$, gas phase $\rho = 0.36$, mf $\rho = 0.82$.

the gas phase to an mf value of 0.17. Accordingly, the maximum of the absorption blueshifts, slightly reducing the exciton shift. Similar considerations apply to the dye in the middle panels, whose ionicity is reduced from 0.64 in the gas phase to 0.5 in the mf approach. For $\rho = 0.5$ (the cyanine limit) the Condon vibrational coupling (proportional to the squared mesomeric dipole moment) vanishes, leading to the disappearance of the vibronic structure in the absorption and fluorescence bands. More inspiring is the case of the zwitterionic dye in the right column of Fig. 3. Here the decrease of the ionicity from 0.76 in the gas phase to 0.61 in the mf approximation is responsible for a large red-sfift of the absorption band. Taking as proper reference the mf frequency, a blue-shift of the absorption band is observed for the aggregate, fully in line with its H character, as due to repulsive ($V > 0$) intermolecular interactions.

Fluorescence in H-aggregates comes from electronic states at the border of the Brillouin zone and are therefore only allowed due to the coupling to vibrational modes. As a result, very weak and largely red-shifted bands are observed, but what we notice here is that, since the dominating (Condon) term accounting for vibronic coupling vanishes in the cyanine limit, the fluorescence intensity is vanishingly small in this limit.

A similar analysis applies to the aggregates in Fig. 4, corresponding to the case of weak attractive intermolecular interactions ($V = -1$). Intense emission bands and vanishing Stokes shifts in the aggregate are fully in line with J-aggregate behavior. The redshift of absorption (and emission) bands observed for the dyes in the left and middle panels of Fig. 4 is again in line with J-aggregate behavior. The most striking result however is recognized again for the most polar molecule ($\rho = 0.36$ in the gas phase) in the right panels of Fig. 4: here in fact the exciton band moves to the blue with respect to the gas-phase molecule.

But again this anomalous behavior is simply related to the choice of a wrong reference. In the aggregate, the mf solution of the problem drives the molecule deep in the ionic regime with $\rho = 0.82$. This implies a large blue shift of the absorption and fluorescence bands, so that, when taking as a reference the gas phase molecule, an apparent blue-shift of the exciton band is observed, that actually corresponds to a red-shift when the proper mf reference is considered, in line with the attractive nature of the interactions. We also notice that for the zwitterionic system, when the wrong reference state is considered, the intensity of the transitions (both absorption and fluorescence) decreases and the vibronic structure becomes more prominent, in striking contrast with the J-nature of the aggregate. This inconsistency is however quite naturally solved if the proper mf reference is considered: in all cases the spectral intensity increases when going from the mf dye to the aggregate, while the vibronic structure becomes less and less prominent. Quite interestingly, results in the central panel of Fig. 4 refer to a dye with ionicity $\rho = 0.16$ in the gas phase that is driven to the cyanine limit, $\rho = 0.50$, when embedded in the aggregate. Once again, in the cyanine limit the vibronic structure of the absorption and fluorescence bands disappears.

3.2 Medium and strong coupling

We will now address the cases of medium and strong coupling. Fig. 5 shows the absorption spectra calculated for H-aggregates in the medium ($V = 1.6$) and strong-coupling ($V = 2.0$) regimes. It turns out that $N_e = 4$ is the minimum number of exciton states to be introduced to obtain convergence. Indeed, $N_e = 3$ results are in general untenable, with the only exception of the system in the central panel of Fig. 5 with mf ionicity $\rho = 0.5$. In this case in fact all terms in eqn (6) proportional to $1 - 2\rho$ vanish. Accordingly, the vibronic structure disappears, as

This journal is © the Owner Societies 2021

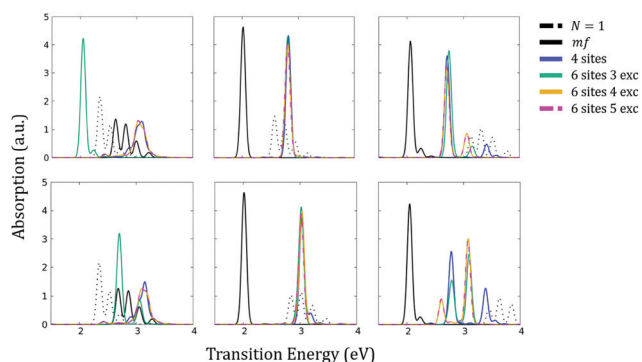Phys. Chem. Chem. Phys., 2021, 23, 8282–8291 | 8287

Fig. 5 H aggregate absorption spectra. All results refer to a system with $\varepsilon_v = 0.4$ and $\omega_v = 0.17$. Top panels show results for $V = 1.6$, from left to right: $z_0 = 0.8$, gas phase $\rho = 0.21$, mf $\rho = 0.15$; $z_0 = -0.6$, gas phase $\rho = 0.84$, mf $\rho = 0.5$; $z_0 = -1.0$, gas phase $\rho = 0.9$, mf $\rho = 0.62$. Bottom panels show results for $V = 2.0$, from left to right: $z_0 = 0.8$, gas phase $\rho = 0.21$, mf $\rho = 0.14$; $z_0 = -0.8$, gas phase $\rho = 0.88$, mf $\rho = 0.5$; $z_0 = -1.2$, gas phase $\rho = 0.92$, mf $\rho = 0.61$.

discussed above, but also all terms related to the mesomeric dipole moment (the difference between the permanent dipole moments in the excited and ground states) vanish. For the electronic part, the Hamiltonian in the $\rho = 0.5$ limit reduces to that relevant to a non-polar aggregate and most of the anomalous effects associated with aggregates of polar and polarizable dyes are washed out.[43] Once convergence is reached, finite size effects are marginal for largely neutral dyes, as well as for dyes in the cyanine limit, but become relevant for zwitterionic dyes.

More interesting is the case of J-aggregates, where electrostatic intermolecular interactions lead to intriguing phenomena.[31,32] Fig. 6 shows absorption and fluorescence spectra calculated for a system with $V = -1.6$, corresponding to the

curve in Fig. 2f that marks the boundary between the normal (weak coupling) and the bistable (strong coupling) regimes. Much as in the weak coupling case, the apparently anomalous behavior observed when comparing aggregate spectra with spectra calculated for the isolated dye is relieved if the proper reference system is considered, corresponding to the mf solution. In all cases in fact the aggregate spectrum is red-shifted with respect to the relevant mf spectrum. The most important difference with respect to the weak coupling is the appearance of finite size effects, with $N = 6$ results differing from $N = 4$, pointing to largely delocalized excitons. Moreover, to obtain convergence for $N = 6$, at least $N_e = 4$ is needed (see Fig. S1, ESI†), in sharp contrast with the weak coupling case. Quite interestingly, finite size effects are marginal for the system described in middle column of Fig. 6 where the mf ionicity is 0.5. As discussed above, in this limit, the vanishing of terms proportional to $1 - 2\rho$ not only kills the main vibronic coupling term, but also reduces the electronic part of the Hamiltonian to that of aggregates of non-polar dyes.

This is even more evident in the strong coupling limit in Fig. 7, showing spectra calculated for $V = -2.0$. Similar considerations apply as in the medium-coupling regime, but in this case $N = 6$ results do not converge until the maximum number of excitons $N_e = 6$ is accounted for in the calculation, or in other terms, until the complete electronic basis is considered (see Fig. S2, ESI†). This immediately tells us that the exciton–exciton interaction term (the first term in the last line of eqn (6)) lowers the energy of multiexciton states that get mixed with the lowest excited states giving a sizable multiexcitonic character to the state, as extensively discussed in ref. 31 and 32. Again, this term vanishes for a system with an mf ionicity $\rho = 0.5$, so that for this system (the middle panels of Fig. 7) the $N = 6$ results already converge at $N_e = 3$.
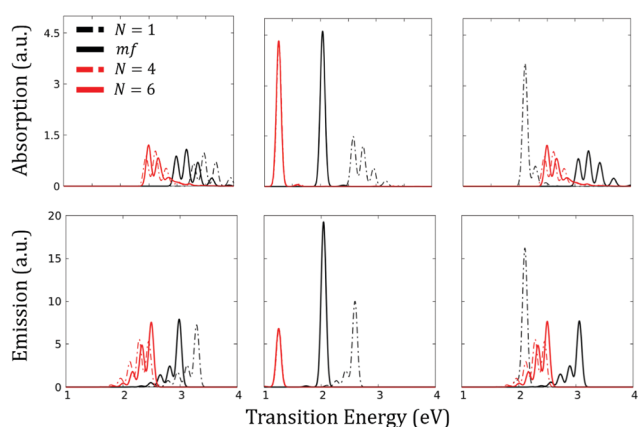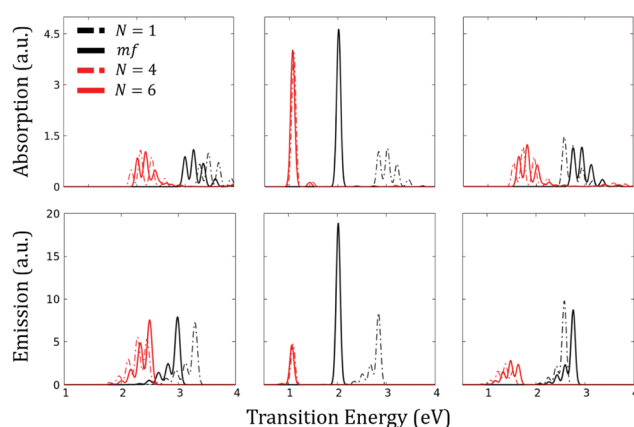

Fig. 6 J aggregate, $V = -1.6$, $\varepsilon_v = 0.4$, $\omega_v = 0.17$: top and bottom panels show the calculated absorption and fluorescence spectra. Intensities per molecule are reported in arbitrary units. Left panels refer to a system with $z_0 = 1.5$, corresponding to an ionicity for the isolated dye $\rho = 0.09$ that increases in the mf approximation to $\rho = 0.10$. Middle panels: $z_0 = 1.0$, gas phase $\rho = 0.16$, mf $\rho = 0.50$. Right panels: $z_0 = 0.5$, gas phase $\rho = 0.33$, mf $\rho = 0.90$.

Fig. 7 J aggregate, $V = -2.0$, $\varepsilon_v = 0.4$, $\omega_v = 0.17$: top and bottom panels show the calculated absorption and fluorescence spectra. Intensities per molecule are reported in arbitrary units. Left panels refer to a system with $z_0 = 1.5$, corresponding to an ionicity for the isolated dye $\rho = 0.09$ that increases in the mf approximation to $\rho = 0.11$. Middle panels: $z_0 = 1.2$, gas phase $\rho = 0.12$, mf $\rho = 0.50$. Right panels: $z_0 = 1.0$, gas phase $\rho = 0.16$, mf $\rho = 0.87$.

4 Discussion

Extending previous work[31] to account for molecular vibrations, as needed to properly address spectral bandshapes, here we propose a two-step approach for the description of optical spectra of aggregates of polar and polarizable molecules. The first step is the definition of the proper reference state as the mf solution of the problem. Basically, the ground state polarity of each dye is self-consistently defined by the polarity of the surrounding dyes, leading to increased polarity for attractive intermolecular interactions and reduced polarity for repulsive interactions. Of course all molecular properties (including transition frequencies and dipole moments) are affected by this variation. The mf state defines the proper reference state for the exciton model. The molecular geometry is also affected by the molecular polarity and the correct reference state for the vibrational problem is defined *via* a Lang–Firsov transformation that translates the origin of the vibrational coordinates to the equilibrium position relevant to the charge distribution of the molecule inside the aggregate. Since molecular vibrations in turn affect the molecular polarity, vibronic coupling leads to another self-consistent interaction. While this may look like a difficult problem, it boils down to a simple self-consistent diagonalization of a two by two Hamiltonian.[39,42]

The essential state model adopted here has been extensively validated against experiment and describes in a very effective way the low-energy spectral properties of push–pull dyes accounting for the environmental effects in solution,[34–36] aggregates,[33,42] films[44] and crystals.[39,48] In the context of this work, we underline that the model relies on similar approximations as the standard exciton model, accounting for a single electronic excitation and a single vibrational mode per molecule. At variance with the standard exciton model, however, the proposed model fully accounts for the molecular polarizability and for the dependence of the ground and excited state molecular geometry on the molecular polarity.

Once the proper reference state is defined, several interaction terms are recognized in the Hamiltonian that can be classified as excitonic, when conserving the exciton number, and ultraexcitonic when mixing states with a different number of excitons.[31] The vibrational coupling leads to an excitonic term that corresponds to the Condon coupling in the exciton model. This term is proportional to $1 - 2\rho$, and vanishes in systems whose mf ionicity is close to 0.5: in these systems the vibronic bandshape is washed out. The ultraexcitonic term exchanges vibrational quanta and excitons and has marginal spectroscopic effects in the weak coupling limit as shown in Fig. 8 and 9 that compare the exact results obtained in the weak and strong coupling regimes for H and J aggregates with those obtained suppressing the non-Condon vibronic coupling in the Hamiltonian in eqn (6). Non-Condon corrections give rise to sizable effects in the strong regime.

As for excitonic terms originating from electrostatic interactions, we recognize terms $\propto \rho(1 - \rho)$, *i.e.* proportional to the squared transition dipole moment of the mf molecules: these terms are responsible for the exciton hopping. Other terms
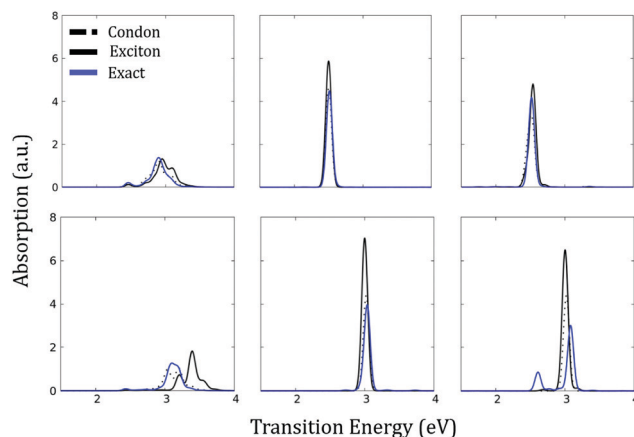

Fig. 8 H-aggregates with $N = 6$. Top panels show weak-coupling results, $V = 1$ for the same values of model parameters as in Fig. 3; bottom panels show results for strong coupling, $V = 2$, for the same parameters as in the bottom panels of Fig. 5. In all panels blue lines show converged results for the total Hamiltonian, dashed black curves show results obtained neglecting the non-Condon electron-vibration coupling term, and continuous black lines show results for the exciton model, *i.e.* suppressing all ultraexcitonic terms in the Hamiltonian.

appear proportional to the mesomeric dipole moment $(1 - 2\rho)$ that account for exciton–exciton interactions. These last terms vanish when the mf molecular ionicity is close to 0.5, and the system reduces to an aggregate of non-polar dyes. The exciton approximation works reasonably well for weak coupling, but fails in the strong coupling regimes (see Fig. 8 and 9).

Indeed, with increasing coupling, ultraexciton terms enter into play with particularly impressive effects in J-aggregates, where bistability regions are observed in the mf solution.[31,32] Finite size effects become important in these conditions and the exciton basis cannot be broken down to account for just the
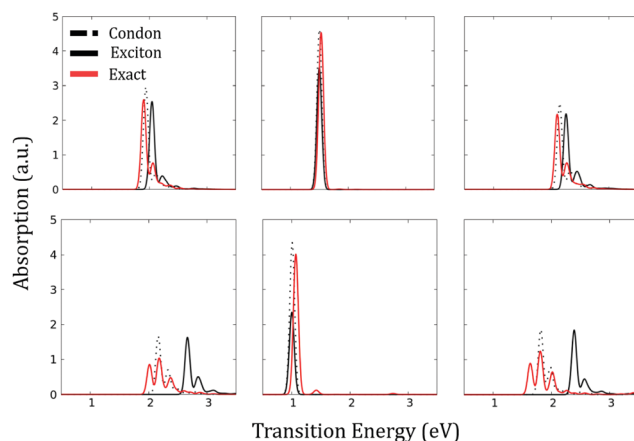

Fig. 9 J-aggregates with $N = 6$. Top panels show weak-coupling results, $V = -1$ for the same values of model parameters as in Fig. 4; bottom panels show results for strong coupling, $V = -2$, for the same parameters as in Fig. 7. In all panels blue lines show converged results for the total Hamiltonian, dashed black curves show results obtained neglecting the non-Condon electron-vibration coupling term, and continuous black lines show results for the exciton model, *i.e.* suppressing all ultraexcitonic terms in the Hamiltonian.

This journal is © the Owner Societies 2021

Phys. Chem. Chem. Phys., 2021, **23**, 8282–8291 | **8289**

first few exciton states (up to 3 excitons are enough to obtain converged results in the weak coupling limit). Indeed, the lowest excited state in these conditions cannot be described, not even approximately, as a state with a single exciton; instead it corresponds to a state where several excited molecules cluster together in a multiexciton state.[31,32]

In this work we only consider perfectly ordered 1D aggregates. Accordingly, translational symmetry is exploited to successfully address the fairly complex problem of coupled electronic and vibrational motions in fairly large systems. Modest disorder effects are expected in crystalline systems, but they are important for aggregates in solution. Molecular dynamics and more generally multiscale approaches are powerful tools for addressing disorder that occurs in aggregates in solution[49,50] as related to the conformational motion of the aggregate itself, as well as to the fluctuating electric field associated with polar solvation. However, treating electronic and vibrational degrees of freedom using a truly non-adiabatic approach is challenging for large disordered systems, and requires the development of new approximation techniques. In this respect, the proposed two-step approach to aggregates of polar dyes may offer a good starting point towards the development of few-particle approaches, that are successfully exploited for aggregates of non-polar dyes.[7,17,22,25]

5 Conclusions

The spectroscopic effects of intermolecular interactions have attracted the interest of scientists for almost a century. The exciton model, neglecting intermolecular interactions among non-degenerate states, offers a simple and effective approach for understanding the spectral properties of molecular crystals and aggregates.[7,14,15] However, it must be recognized that the model fully neglects the molecular polarizability,[31] in the assumption that the nature of the ground state is not altered by intermolecular interactions. This approximation works fairly well in aggregates of non-polar molecules, where the molecular polarizability shows up mainly as a variation of the spectral intensities,[25] an effect that is difficult to assess experimentally. In aggregates of polar molecules, however, the large electric fields generated by the nearby polar molecules affect the state of polarizable dyes considerably, leading to two major effects. In the first place, when a polar and polarizable molecule is surrounded other similar molecules, it will readjust its polarity in response to the electrical potential generated by the charges in the surrounding molecules. Accordingly, the nature of the molecules will change, with the ground state polarity at equilibrium being reduced in H-aggregates with respect to the isolated molecule and increased in J-aggregates. Of course, the equilibrium geometry of the molecule will readjust accordingly. To properly rationalize aggregation effects it is important to take into account this mean-field effect, building the model for interacting dyes starting from the proper reference. This allows the singling out of excitonic and ultraexcitonic effects for properly addressing vibrational coupling and hence vibronic band-shapes. Specifically, the anomalous red/blue shifts observed in H/J aggregates when the

reference state is taken to correspond to the isolated molecule, turn out to be normal blue/red shifts when the proper reference is taken as the molecule in its environment. Similar anomalous effects on band-shapes are also easily sorted out, at least in the weak-coupling regime. Apart from a better understanding of the physics of these intriguing systems, the proper choice of the reference state gives an enormous computational advantage: for not too large couplings in fact it is possible to truncate the electronic basis only accounting for states with a limited number of excitons. This is particularly important because the non-adiabatic basis, needed to properly address the aggregate, increases very fast with the number of states. Our approach, that also accounts for the translational symmetry in aggregates with periodic boundary conditions, allowed us to diagonalize exactly non-adiabatic Hamiltonian for systems with up to 6 molecules. Reaching large aggregates is important for singling out the finite size effects that are particularly interesting for J aggregates in the medium-large coupling regime, where the low-lying excitations acquire a multiexciton character, corresponding to a droplet of excited states bound together by attractive intermolecular interactions. In this paper we only considered linear absorption and fluorescence spectra, but our approach can easily address non-linear optical spectra, where important aggregation effects are expected.

Conflicts of interest

There are no conflicts to declare.

Acknowledgements

Notes and references

1 T. Förster, *Modern Quantum Chemistry*, Academic Press, 1965, p. 93.
2 G. D. Scholes, *Annu. Rev. Phys. Chem.*, 2003, **54**, 57–87.
3 F. Di Maiolo and A. Painelli, *J. Chem. Theory Comput.*, 2018, **14**, 5339–5349.
4 M. Anzola, C. Sissa, A. Painelli, A. A. Hassanali and L. Grisanti, *J. Chem. Theory Comput.*, 2020, **16**, 7281–7288.
5 D. P. Craig and S. H. Walmsley, *Excitons in Molecular Crystals*, Benjamin, 1968.
6 J. Knoester, *Organic Nanostructures: Science and applications*, IOS Press, *Amsterdam*, 2002, vol. 149, pp. 149–186.
7 N. J. Hestand and F. C. Spano, *Chem. Rev.*, 2018, **118**, 7069–7163.

8290 | *Phys. Chem. Chem. Phys.*, 2021, **23**, 8282–8291

This journal is © the Owner Societies 2021

8 J. R. Lakowicz, *Principles of Fluorescence Spectroscopy*, Springer, US, 1999, p. 698.

9 B. Valeur and M. N. Berberan-Santos, *Molecular Fluorescence: Principles and Applications*, Wiley-VCH Verlag GmbH & Co. KGaA, 2012.

10 M. J. Rice, *Phys. Rev. Lett.*, 1976, **37**, 36–39.

11 A. Painelli and A. Girlando, *J. Chem. Phys.*, 1986, **84**, 5655–5671.

12 M. Souto, J. Guasch, V. Lloveras, P. Mayorga, J. T. L. Navarrete, J. Casado, I. Ratera, C. Rovira, A. Painelli and J. Veciana, *J. Phys. Chem. Lett.*, 2013, **4**, 2721–2726.

13 N. J. Hestand, C. Zheng, A. R. Penmetcha, B. Cona, J. A. Cody, F. C. Spano and C. J. Collison, *J. Phys. Chem. C*, 2015, **119**, 18964–18974.

14 M. Kasha, *Radiat. Res.*, 1964, **3**, 317–331.

15 A. S. Davidov, *Theory of Molecular Excitons*, Plenum Press, 1971.

16 V. M. Agranovich and M. D. Galanin, *Excitons in Molecular Crystals*, North-Holland, 1982.

17 F. C. Spano, *Acc. Chem. Res.*, 2010, **43**, 429–439.

18 E. U. Condon, *Rev. Mod. Phys.*, 1937, **9**, 432–457.

19 D. P. Craig and T. Thirunamachandran, *Molecular quantum electrodynamics*, Dover, New York, NY, 1998.

20 K. Swathi, C. Sissa, A. Painelli and K. G. Thomas, *Chem. Commun.*, 2020, **56**, 8281–8284.

21 D. Feinberg, S. Ciuchi and F. De Pasquale, *Int. J. Mod. Phys. B*, 1990, **04**, 1317–1367.

22 M. Hoffmann and Z. G. Soos, *Phys. Rev. B: Condens. Matter Mater. Phys.*, 2002, **66**, 024305.

23 F. C. Spano and H. Yamagata, *J. Phys. Chem. B*, 2011, **111**, 5133–5143.

24 A. Painelli, *Chem. Phys.*, 1999, **245**, 185–197.

25 M. Anzola, F. D. Maiolo and A. Painelli, *Phys. Chem. Chem. Phys.*, 2019, **21**, 19816–19824.

26 G. D'Avino, F. Terenziani and A. Painelli, *ChemPhysChem*, 2007, **8**, 2433–2444.

27 S. Sanyal, A. Painelli, S. K. Pati, F. Terenziani and C. Sissa, *Phys. Chem. Chem. Phys.*, 2016, **18**, 28198–28208.

28 B. Bardi, C. Dall'Agnese, K. I. Moineau-Chane Ching, A. Painelli and F. Terenziani, *J. Phys. Chem. C*, 2017, **121**, 17466–17478.

29 C. Zheng, C. Zhong, C. J. Collison and F. C. Spano, *J. Phys. Chem. C*, 2019, **123**, 3203–3215.

30 B. Bardi, C. Dall'Agnese, M. Tassé, S. Ladeira, A. Painelli, K. I. Moineau-Chane Ching and F. Terenziani, *ChemPhotoChem*, 2018, **2**, 1027–1037.

31 F. Terenziani and A. Painelli, *Phys. Rev. B: Condens. Matter Mater. Phys.*, 2003, **68**, 165405.

32 A. Painelli and F. Terenziani, *J. Am. Chem. Soc.*, 2003, **125**, 5624–5625.

33 F. Terenziani, G. D'Avino and A. Painelli, *ChemPhysChem*, 2007, **8**, 2433–2444.

34 A. Painelli, *Chem. Phys. Lett.*, 1998, **285**, 352–358.

35 A. Painelli and F. Terenziani, *J. Phys. Chem. A*, 2000, **104**, 11041–11048.

36 B. Boldrini, E. Cavalli, A. Painelli and F. Terenziani, *J. Phys. Chem. A*, 2002, **106**, 6286–6294.

37 Z. G. Soos and D. J. Klein, *Molecular Association: Including Molecular Complexes*, Academic Press, New York, 1975, vol. 1.

38 A. Girlando and A. Painelli, *Phys. Rev. B: Condens. Matter Mater. Phys.*, 1986, **34**, 2131–2139.

39 J. Guasch, L. Grisanti, S. Jung, D. Morales, G. D'Avino, M. Souto, X. Fontrodona, A. Painelli, F. Renz, I. Ratera and J. Veciana, *Chem. Mater.*, 2013, **25**, 808–814.

40 G. D'Avino, A. Painelli and Z. Soos, *Crystals*, 2017, **7**, 144.

41 F. Terenziani and A. Painelli, *J. Lumin.*, 2005, **112**, 474–478.

42 S. Sanyal, C. Sissa, F. Terenziani, S. K. Pati and A. Painelli, *Phys. Chem. Chem. Phys.*, 2017, **19**, 24979–24984.

43 C. Zhong, D. Bialas and F. C. Spano, *J. Phys. Chem. C*, 2020, **124**, 2146–2159.

44 F. Terenziani, A. Painelli, A. Girlando and R. M. Metzger, *J. Phys. Chem. B*, 2004, **108**, 10743–10750.

45 D. K. A. P. Huu, C. Sissa, F. Terenziani and A. Painelli, *Phys. Chem. Chem. Phys.*, 2020, **22**, 25483–25491.

46 A. Painelli and F. Terenziani, *Chem. Phys. Lett.*, 1999, **312**, 211–220.

47 H. Nakanotani, T. Higuchi, T. Furukawa, K. Masui, K. Morimoto, M. Numata, H. Tanaka, Y. Sagara, T. Yasuda and C. Adachi, *Nat. Commun.*, 2014, **5**, 4061.

48 G. D'Avino, L. Grisanti, J. Guasch, I. Ratera, J. Veciana and A. Painelli, *J. Am. Chem. Soc.*, 2008, **130**, 12064–12072.

49 A. Segalina, X. Assfeld, A. Monari and M. Pastore, *J. Phys. Chem. C*, 2019, **123**, 6427–6437.

50 M. Eskandari, J. C. Roldao, J. Cerezo, B. Milián-Medina and J. Gierschner, *J. Am. Chem. Soc.*, 2020, **142**, 2835–2843.